Fault permeability models for geothermal doublet designs

Jan ter Heege[1]

[1] TNO, Princetonlaan 6, 3584 CB, Utrecht, the Netherlands

Jan.terHeege@tno.nl

Keywords: faults and fractures, 3D permeability, geothermal doublets, optimum designs.

ABSTRACT

The occurrence and properties of natural faults and fractures in geothermal reservoirs are key in determining reservoir flow properties, and thereby the performance of geothermal doublets placed in fractured reservoirs or in the vicinity of fault zones. In this paper, an analytical model is presented that describes the 3D non-isotropic permeability of a geothermal reservoir around a major fault zone, taking into account typical fault architectures consisting of a fault core, a damage zone and surrounding intact reservoir matrix. The sensitivity of model predictions to orientations of sedimentary layers, damage zone fractures and fault core is analysed for typical permeability contrasts and dimensions of intact reservoir, damage zone fractures and fault core. The model can be used to determine optimum orientation of geothermal doublets around fault zones, taking into account the distribution and characteristics of faults, fractures and sedimentary layering. Implications for optimizing the design of geothermal doublets placed in the vicinity of large fault zones are given.

1. INTRODUCTION

The occurrence and properties of natural faults in geothermal reservoirs are key in determining reservoir flow properties, and thereby the success of many geothermal projects (Hickman et al 1997; Fairly and Hinds 2004; Faulds et al. 2010; Moeck 2014). Accordingly, exploration for new geothermal sites will benefit from site-specific data on fault-related factors like damage zone fracture density, connectivity and permeability. In most cases, such data is lacking during geothermal exploration, but existing knowledge can be used to constrain typical fault zone architectures, spatial distribution of permeability and characteristics of damage zone fracture populations.

The characteristics of natural fault zones can vary widely depending on local geological and tectonic settings (Kim et al 2004; Wibberley et al 2008; Faulkner et al 2010). Site-specific characteristics of fault and fracture populations have been determined using seismic surveys, outcrop analogues, core material, and laboratory experiments (Odling et al 1999; Bonnet et al 2001; Torabi and Berg 2011). These studies have provided some generic fault scaling relations that can be used to constrain fault zone characteristics, such as damage zone width, fracture density and dominant fracture orientation. Accordingly, typical fault zone permeability models can be constructed even if site-specific (subsurface) data on fault zone characteristics is lacking.

The relationship between fluid flow and faulting has been studied extensively (Frank 1965; Sibson 1981; Caine et al 1996; Fisher and Knipe 2001). Most fault zones consists of a specific architecture with different structural units, i.e. a single or multiple fault cores and damage zones, surrounded by intact reservoir rock (Chester and Logan 1986; Wibberley et al 2008; Faulkner et al 2010). Permeability may vary considerably in each of these structural units, and the characteristic architecture of a fault zone will determine the permeability in and around fault zones (Barton et al 1995; Wibberley and Shimamoto 2003; Mitchell and Faulkner 2012).

Although many studies that model the permeability around fault zones address some aspects of fault architecture (Yielding et al 1997; Brown and Bruhn 1998; Odling et al 2004), few consider 3D permeability in all structural units. Moreover, one dominant fracture set with equally-spaced fractures is often assumed to describe fractured media such as damage zones (Pickup et al 1995; Lei et al 2015), hence ignoring relations between the orientation of main faults and damage zone fractures (Tchalenko 1970; Kim et al 2004) and spatial variation in fracture density (Mitchell and Faulkner 2012). Another major challenge for application to fault-controlled geothermal energy resources is the general lack of site-specific data on fault and fracture populations.

In this study, an analytical model has been derived for the permeability of a geothermal reservoir around a major fault zone. The model is based on a fractured shale permeability model by Ter Heege (2016), and is modified to be applicable to geothermal energy extraction around fault zones. Fault zones are modelled with a typical architecture consisting of 3 structural units, i.e. a fault core, a damage zone and surrounding intact reservoir matrix. Permeability is modelled using 3D permeability tensors that describe

non-isotropic permeability in each of the structural units. Permeability of intact reservoir rock includes anisotropy due to sedimentary layering. Damage zone permeability is based on fracture density and orientation, and includes the effect of decreasing fracture density with increasing distance from the fault core. The permeability of the fault core can include anisotropy due to fabric in the fault gouge. Bulk permeability can be described by combining permeability of the fault core, damage zone and intact reservoir including typical dimensions of each structural unit as well as distance and orientation between geothermal doublets.

The bulk permeability model can be used to analyse the geothermal power for a doublet system consisting of a surface heat exchanger, an injection well (“injector”) and a production well (“producer”) that is placed in the vicinity of a fault zone. Implications for the optimum design of geothermal doublet systems placed around fault zones are discussed. It is shown that produced geothermal power can be considerably enhanced if doublets are placed in optimum orientation with respect to existing damage zone fracture populations. Therefore, optimization of geothermal doublet designs in geothermal reservoirs that are crosscut by fault zones help de-risking geothermal exploration and exploitation.

2. MODEL FOR FAULT-CONTROLLED RESERVOIR PERMEABILITY

Fault zones are modelled with a typical architecture consisting of 3 structural units, i.e. a fault core, a damage zone and surrounding intact reservoir matrix (Fig. 1, c.f. Ter Heege 2016). Dimensions of fault zone and its structural components are constrained by length along the fault strike (L), length along fault dip (S), displacement along fault dip (D_S), damage zone width (W_D), damage zone fracture width (W_F), and fault core width (W_C). Anisotropic permeability in each of the units is described using 3D permeability tensors ($\boldsymbol{K}^*$) that are defined in terms of 3 orthogonal principal permeabilities in different coordinate systems.

$$\boldsymbol{K}^* = \begin{pmatrix} K_{11}^* & 0 & 0 \\ 0 & K_{22}^* & 0 \\ 0 & 0 & K_{33}^* \end{pmatrix} \qquad [1]$$

The asterisk in equation [1] is included to acknowledge that the principal permeabilities are defined using different Cartesian coordinate systems for the different structural units (following the right-hand rule for axes orientations).

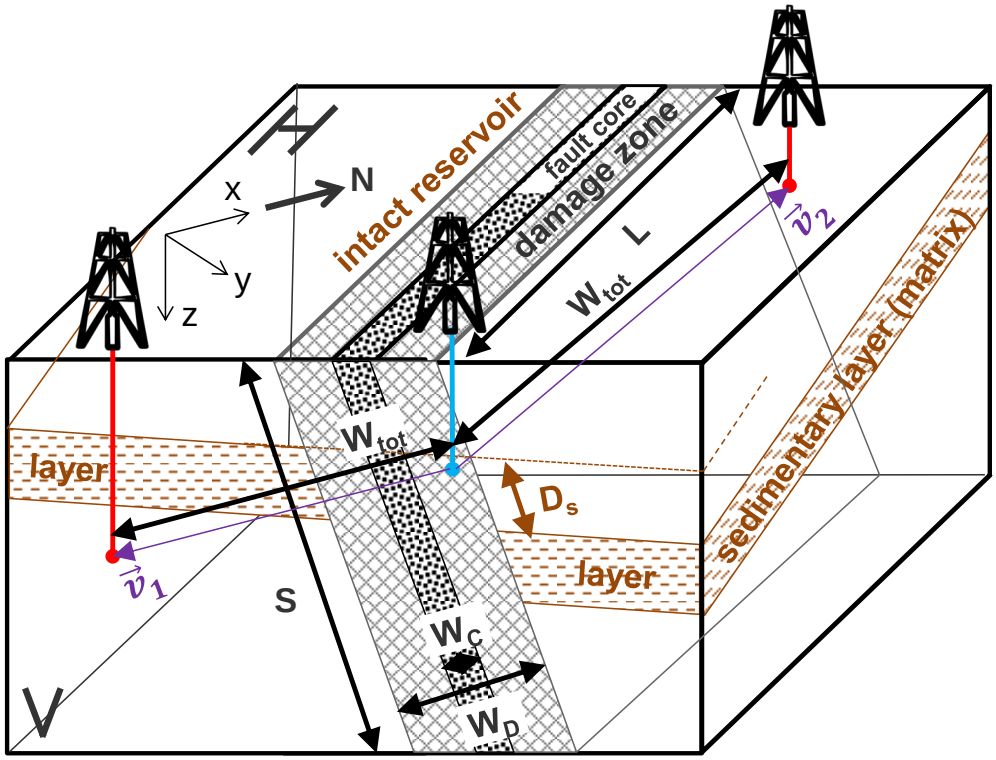

Figure 1: Schematic diagram of simplified fault zone showing the structural units (i.e. non-fractured intact shale matrix with sedimentary layers, damage zone and fault core), and dimensions used in the fractured shale permeability model (*L*- length along fault strike, *S*- length along fault dip, D_S- displacement along fault dip, W_D- damage zone width, W_C- fault core width, W_{tot} – distance between injector and producer doublet wells, v_x- orientation of geothermal doublet injector-producer). The geographical coordinate system (axis x, y, z in northern, eastern and depth direction, respectively) is also indicated.

Permeability tensors are transformed between the different coordinate systems by tensor transformations using a rotation matrix $\boldsymbol{R}$ for a full Euler rotation based on the orientations of principal permeabilities relative to matrix layers, fault core and damage zone.

The matrix permeability tensor ($\boldsymbol{K}^* = \boldsymbol{K_M}'$) is defined on the basis of sedimentary layers that may be present in the intact reservoir at an orientation described by the dip direction (θ_M) and dip (φ_M). The following orientations of principle permeabilities are assumed: (1) K_{M11}' is within the layers at an angle ω_M relative to θ_M, (2) K_{M22}' is within the layers perpendicular to K_{M11}', and (3) K_{M33}' is perpendicular to the layers in downward direction. Together, the principle permeabilities define a layer-based coordinate system. The matrix permeability tensor and layer-based coordinate system can account for effects of sedimentary structures such as cross-bedding (i.e. by specifying ω_M and K_{M11}'/K_{M22}') and permeability anisotropy due to bedding (i.e. by specifying K_{M11}'/K_{M33}').

The damage zone permeability tensor ($\boldsymbol{K}^* = \boldsymbol{K_D}''$) is defined on the basis of a dominant fracture set that may be present in the damage zone at an orientation described by the dip direction (θ_F) and dip (φ_F). The following orientations of principle permeabilities are assumed: (1) K_{F11}''' is parallel to the normal vector of fracture planes for the dominant fracture set, (2) K_{F22}''' is parallel to the layer strike, and (3) K_{F33}''' is parallel to the layer dip vector. Together, the principle permeabilities define a fracture-based coordinate system. The principle damage zone permeabilities are expressed as a combination of matrix permeability ($\boldsymbol{K_M}'''$, now in the fracture-based coordinate system) and damage zone fracture permeability ($\boldsymbol{K_F}'''$). The damage zone permeability tensor and fracture-based coordinate system can account for effects of permeability anisotropy in the fractures (i.e. by specifying K_{F11}''', K_{M22}''' and K_{M33}'''), different fracture orientations (i.e. by specifying θ_F and φ_F), and different fracture densities. Damage zone permeability perpendicular to the fracture plane (K_{D11}''') is calculated using the harmonic mean of diagonal tensor components (K_{M11}''' and K_{F11}'''), while damage zone permeability parallel to the fracture plane (K_{D22}''' and K_{D33}''') is calculated by the arithmetic mean of K_{M22}''' and K_{F22}''' and K_{M33}''' and K_{F33}''', respectively. As off-diagonal tensor components of $\boldsymbol{K_F}'''$ are zero per definition, the off-diagonal components of $\boldsymbol{K_D}'''$ that govern cross-flow are based on $\boldsymbol{K_M}'''$ (e.g., Pickup et al., 1995).

$$K_{D11}''' = \left(\frac{F_w W_F}{K_{F11}'''} + \frac{(1 - F_w W_F)}{K_{M11}'''} \right)^{-1} \qquad [2a]$$

$$K_{D22}''' = F_w W_F K_{F22}''' + (1 - F_w W_F) K_{M22}''' \qquad [2b]$$

$$K_{D33}''' = F_w W_F K_{F33}''' + (1 - F_w W_F) K_{M33}''' \qquad [2c]$$

$$K_{Dij}''' = (1 - F_w W_F) K_{Mij}''' \text{ for } i \neq j \qquad [2d]$$

Where the contribution of matrix and damage zone fractures to damage zone permeability is weighted using damage zone fracture width (W_F) and density of fractures in the damage zone (F_w). Fracture density decreases with increasing distance (w) from the center of the fault core (c.f. Mitchell and Faulkner, 2012).

$$F_w = F_C \, exp\left(\frac{w - W_C}{w - W_D} \right) \text{ with } W_c \leq w \leq W_D \quad [3]$$

Where distance from the fault core is normalized to give fracture density $F_w = F_C$ at the outer edge of the fault core ($w = W_C$) where permeability equals that of the fault gouge, and $F_w \rightarrow 0$ at the outer edge of the damage zone ($w \rightarrow W_D$) where permeability equals that of the matrix. It is assumed that one dominant set controls permeability, but the model may be extended to include multiple fracture sets as frequently observed in fault zones (Tchalenko, 1970; Kim et al., 2004).

The fault core permeability tensor ($\boldsymbol{K}^* = \boldsymbol{K_C}''$) is defined on the basis of the dominant fault zone orientation described by the dip direction (θ_C) and dip (φ_C) of the fault core. The following orientations of principle permeabilities are assumed: (1) K_{C11}'' is parallel to the normal of the main fault plane through the fault core, (2) K_{C22}''' is parallel to the strike of the main fault plane, and (3) K_{C33}''' is parallel to the dip vector of the main fault plane. Together, the principle permeabilities define a fault-based coordinate system. The fault core permeability tensor and fault-based coordinate system can account for effects of permeability anisotropy in the fault core (i.e. by specifying K_{C11}''', K_{C22}''' and K_{C33}''').

The principle bulk permeabilities around a single fault zone are determined in the fault-based coordinate system ($\boldsymbol{K_B}''$) by combining matrix permeability ($\boldsymbol{K_M}''$), average damage zone permeability ($\boldsymbol{K_D}''$) and fault core permeability ($\boldsymbol{K_C}''$), averaged over the distance (W_{tot}) between the doublet injector and producer. Equations [2] give the permeability tensor components for the damage zone at a distance from the center of the fault core. $\boldsymbol{K_D}''$ is calculated based on the average permeability over distance $w_D = w_{D2} - w_{D1}$ in the damage zone that can be calculated by substituting equation [3] in [2] and integrating local permeability tensor components over w_D.

$$\tilde{K}_{Dij}''' = \frac{1}{w_D} \int_{w_{D1}}^{w_{D2}} K_{Dij}''' dw \qquad [4]$$

Where w_D is determined by the location of the injector and producer relative to fault core and damage zone (c.f. Fig. 1). Bulk permeability perpendicular to the fault core (K_{B11}'') is calculated using the harmonic mean of diagonal tensor components K_{M11}'', K_{D11}'' and K_{C33}''. Bulk permeability parallel to the fracture plane (K_{B22}'' and K_{B33}''') is calculated by the arithmetic mean of K_{M22}'', K_{D22}'', K_{C22}'', and K_{M33}'',

K_{D33}'', K_{C33}'', respectively. As off-diagonal tensor components of $\boldsymbol{K_C}$'' are zero per definition, the off-diagonal components of $\boldsymbol{K_B}$'' that govern cross-flow are based on $\boldsymbol{K_M}$'' and $\boldsymbol{K_D}$''.

$$K''_{B11} = \left(\frac{(W_{tot} - W_D - W_C)}{W_{tot} K''_{M11}} + \frac{W_D}{W_{tot} K''_{D11}} + \frac{W_C}{W_{tot} K''_{C11}} \right)^{-1} \quad [5a]$$

$$K''_{B22} = \frac{(W_{tot} - W_D - W_C) K''_{M22}}{W_{tot}} + \frac{W_D K''_{D22}}{W_{tot}} + \frac{W_C K''_{C22}}{W_{tot}} \quad [5b]$$

$$K''_{B33} = \frac{(W_{tot} - W_D - W_C) K''_{M33}}{W_{tot}} + \frac{W_D K''_{D33}}{W_{tot}} + \frac{W_C K''_{C33}}{W_{tot}} \quad [5c]$$

$$K''_{B1j} = \left(\frac{(W_{tot} - W_D - W_C)}{W_{tot} K''_{M1j}} + \frac{W_D}{W_{tot} K''_{D1j}} \right)^{-1} \quad \text{for } j = 2, 3 \quad [5d]$$

$$K'''_{Bij} = \frac{(W_{tot} - W_D - W_C) K'''_{Mij}}{W_{tot}} + \frac{W_D K''_{Dij}}{W_{tot}} \quad i \neq j; \; i = 2, 3 \quad [5e]$$

The tensor for average bulk permeability ($\boldsymbol{K} = \boldsymbol{K_B}$) is defined with the following orientations of principle permeabilities: (1) K_{B11} is South to North, (2) K_{B22} is West to East, and (3) K_{B33} is downward along depth. Together, the principle permeabilities define a geographical based coordinate system. Dip directions (θ_M, θ_C, θ_F) and dip angles (φ_M, φ_C, φ_F) are defined within the geographical coordinate system. $\boldsymbol{K_B}$ can be derived from $\boldsymbol{K_B}$'' by transformation between the fault-based and geographic coordinate system using a rotation matrix that is based on fault dip direction (θ_C) and dip angle (φ_C). Bulk permeability in the direction between the injector and producer of a doublet (in the geographical coordinate system) can be described by a permeability vector with three components parallel to S-N, W-E and along depth (x-, y- and z-directions, respectively). This vector can be calculated by multiplying $\boldsymbol{K_B}$ with the unit vector ($\vec{v}$) describing the direction between the injector and producer. The average bulk permeability value that can be used to calculate geothermal power for a doublet system is given by the magnitude of the permeability vector, for example following the method outlined by Van Wees et al (2012) for isotropic permeability. It should be emphasized that the current model incorporates fault zone architecture in the description of anisotropic permeability of geothermal reservoirs. Thereby, it can be used to search for optimum doublet designs that yield the best performance in terms of geothermal energy extraction.

3. MODEL SENSITIVITY TO ORIENTATIONS OF LAYERS, FRACTURES AND FAULTS

Model predictions are given for typical permeability contrasts and dimensions of intact reservoir, damage zone fractures and fault core (Table 1).

Table 1: Input parameters for model sensitivity analysis

Parameter	Unit	Value
K_{M11}'	mD	100
K_{M22}'	mD	90
K_{M33}'	mD	10
K_{F11}'''	mD	1000
K_{F22}'''	mD	1000
K_{F33}'''	mD	1000
K_{C11}''	mD	2000
K_{C22}''	mD	2000
K_{C33}''	mD	2000
W_F	m	0.001
W_D	m	100
W_C	m	0.1
W_{tot}	m	1000
F_C	#/m	100

Orientations of fault core, damage zone fractures and reservoir bedding or layering are varied to show the sensitivity of permeability to fault and fracture orientations for each of the structural units (Fig. 2). The example shows values for bulk permeability, assuming that the doublet is oriented in S-N direction ($\vec{v} = [1,0,0]$), and placed in the intact reservoir matrix outside the damage zone or in the damage zone. Accordingly, the variation in bulk permeability results from permeability anisotropy due to layering and density of damage zone fractures, and different orientations of the layers and fractures relative to the doublet.

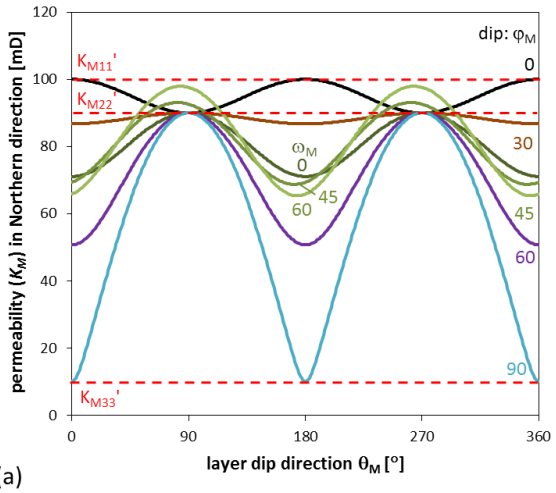

(a)

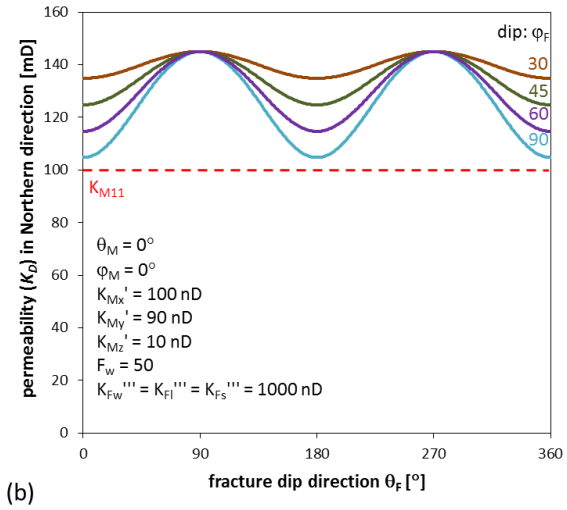

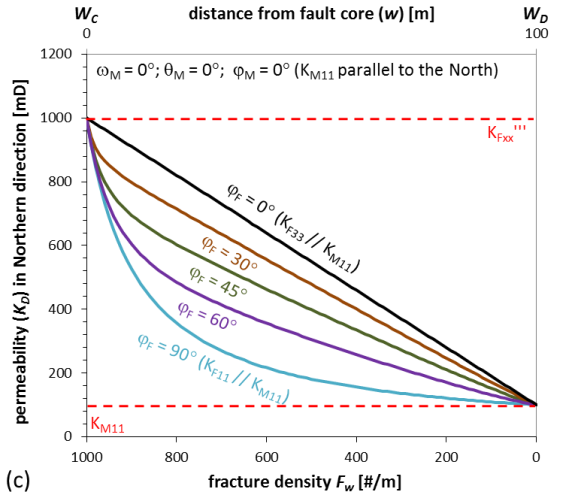

Figure 2: Variation of bulk permeability for a doublet oriented in S-N direction for: (a) different orientations of sedimentary layering in the reservoir (given by layer dip direction θ_M and dip angle φ_M) and largest principal matrix permeability within the matrix layers (ω_M), (b) different orientations of damage zone fractures (given by fracture dip direction θ_D and dip angle φ_D) and F_w = 50, (c) increasing distance from fault core (w) and associated decrease in fracture density (F_w, c.f. Eq. 6). Model input parameters for the sensitivity analysis are given in Table 1.

4. IMPLICATIONS FOR OPTIMIZATION OF GEOTHERMAL DOUBLET DESIGNS AROUND FAULT ZONES

Fluid flow around a fault zone crosscutting a geothermal reservoirs is typically controlled by damage zone fractures or deformation bands (Fossen et al 2007; Mitchell and Faulkner 2012). These structures may give rise to high permeability pathways, for example in geothermal reservoirs with low matrix permeability (e.g., tight sandstone or crystalline rocks) when local deformation is accompanied by dilatation. The permeability contrast used in the example used to analyze model sensitivity (c.f. Fig. 2) is typical of this situation. In the example, high permeability pathways are oriented parallel to the fracture planes. The sensitivity analysis shows that for a doublet oriented in S-N direction, permeability is highest if fractures dip to the West or East (Fig. 2b). The maximum difference in permeability is a factor 1.5 for fractures dipping 90° to the West or East compared to fractures dipping 90° to the North or South in the example. In general, permeability is higher for shallow dipping fractures compared to steeper dipping fractures. Maximum permeabilities occur close to the fault core (Fig. 2c). In contrast, the opposite trends may occur in a geothermal reservoir with high matrix permeability (e.g., porous sandstone or carbonate rocks) where local deformation may be accompanied by compaction resulting in bands of low permeability. If the doublet is placed outside of the damage zone (at $w > 0.5W_D$ from the fault core), permeability difference is mainly determined by the anisotropy caused by the sedimentary layering (Fig. 2a).

If dominant damage zone fractures are at Riedel orientation (R-shear), high permeability pathways resulting from the fractures are oriented at an angle of 45° - φ/2 relative to the fault core (assuming it aligns with direction of maximum shear displacement), and at an angle of -φ/2 relative to the maximum principal stress (c.f. Ter Heege 2016). Hence, structural interpretation of fault patterns or analysis of the stress field aid in determining the optimum orientation of geothermal doublets.

The distribution and characteristics of faults, fractures and sedimentary layering are controlling the performance of geothermal doublets. The optimum orientation of geothermal doublets is dependent on the orientation of sedimentary layers, damage zone fractures and fault core. The presented model, therefore can help optimizing the design of geothermal doublets placed in the vicinity of large fault zones.

It should be emphasized that the choice of optimum drilling location and direction is generally not only motivated by achieving optimum doublet performance, but also by reducing risks of associated with the presence of large faults and fracture networks. Risks may include loss of wellbore stability, screen outs and induced seismicity. Accordingly, optimum orientation of geothermal doublets need to consider optimum doublet performance as well as risks of operations.

3. CONCLUSIONS

In this paper, the permeability of geothermal reservoir around fault zones is studied. The main conclusions can be summarized as follows:

- An analytical model of fault-controlled reservoir permeability is derived that describes

the permeability using 3D permeability tensors for intact reservoir, damage zone and fault core.

- The sensitivity of the model to the orientations of layers, fractures and faults as well as damage zone fracture density is analyzed. It shows that bulk permeability can vary considerably, mainly depending on (i) permeability anisotropy in the matrix, damage zone and fault core, (ii) the orientation of matrix layers and damage zone fractures, and (iii) the location relative to the fault core.

- The model can be used to determine optimum orientation of geothermal doublets around fault zones, taking into account the distribution and characteristics of faults, fractures and sedimentary layering. Thereby, it helps optimizing the design of geothermal doublets placed in the vicinity of large fault zones.

REFERENCES

Barton, C.A., Zoback, M.D. and Moos, D.: Fluid flow along potentially active faults in crystalline rock, *Geology*, **23**, (1995), 683-686.

Bonnet, E., Bour, O., Odling, N.E., Davy, P., Main, I., Cowie, P. and Berkowitz, B.: Scaling of fracture systems in geological media, *Reviews of Geophysics*, **39,** (2001), 347-383.

Brown, S.R. and Bruhn, R.L.: Fluid permeability of deformable fracture networks, *J. Geoph. Res.*, **103**, (1998), 2489-2500.

Caine, J.S., Evans, J.P. and Forster, C.B.: Fault zone architecture and permeability structure, *Geology*, **24**, (1996), 1025-1028.

Chester, F.M. and Logan, J.M.: Implications for mechanical-properties of brittle faults from observations of the Punchbowl fault zone, California, *Pure and Applied Geophysics*, **124**, (1986), 79-106.

Fairly, J.P. and Hinds, J.J.: Rapid transport pathways for geothermal fluids in an active Great Basin fault zone, *Geology*, **32**, (2004), 825-828.

Faulds, J., Coolbaugh, M., Bouchot, V., Moeck, I. and Oğuz, K.: Characterizing Structural Controls of Geothermal Reservoirs in the Great Basin, USA, and Western Turkey: Developing Successful Exploration Strategies in Extended Terranes, *Proceedings World Geothermal Congress 2010*, Bali, Indonesia, (2010), 1-11.

Faulkner, D.R., Jackson, C.A.L., Lunn, R.J., Schlische, R.W., Shipton, Z.K., Wibberley, C.A.J. and Withjack, M.O.: A review of recent developments concerning the structure, mechanics and fluid flow properties of fault zones, *Journal of Structural Geology*, **32**, (2010), 1557- 1575.

Fisher, Q.J. and Knipe, R.J.: The permeability of faults within siliciclastic petroleum reservoirs of the North Sea and Norwegian Continental Shelf, *Marine and Petroleum Geology*, **18**, (2001), 1063-1081.

Fossen, H., Schultz, R.A., Shipton, Z.K. and Mair, K.: Deformation bands in sandstone: a review, *Journal of the Geological Society of London*, **164**, (2007), 755–769.

Frank, F.C.: On dilatancy in Relation to seismic sources, *Reviews of Geophysics*, 3, (1965), 485-503.

Hickman, S.H., Barton, C.A., Zoback, M.D., Morin, R., Sass, J. and Benoit, R.: In-situ stress and fracture permeability along the Stillwater fault zone, Dixie Valley, Nevada, *International Journal of Rock Mechanics & Mining Science*, **34**, (1997), 1-10.

Kim, Y.-S., Peacock, D.C.P. and Sanderson, D.J.: Fault damage zones. *Journal of Structural Geology*, **26**, (2004), 503-517.

Lei, G., Dong, P.C., Mo, S.Y., Yang, S., Wu, Z.S. and Gai, S.H.: Calculation of full permeability tensor for fractured anisotropic media, *Journal of Petroleum Exploration and Production Technology*, **5**, (2015), 1-10.

Mitchell, T.M. and Faulkner, D.R.: Towards quantifying the matrix permeability of fault damage zones in low porosity rocks, *Earth and Planetary Science Letters*, **339–340**, (2012), 24-31.

Moeck, I.: Catalog of geothermal play types based on geologic controls, *Renewable and Sustainable Energy Reviews*, **37**, (2014), 867-882.

Odling, N.E., Gillespie, P., Bourgine, B., Castaing, C., Chiles, J.P., Christensen, N.P., Fillion, E., Genter, A., Olsen, C., Thrane, L., Trice, R., Aarseth, E., Walsh, J.J. and Watterson, J.: Variations in fracture system geometry and their implications for fluid flow in fractures hydrocarbon reservoirs, *Petroleum Geoscience*, **5**, (1999), 373-384.

Odling, N.E., Harris, S.D., and Knipe, R.: Permeability scaling properties of fault damage zones in siliclastic rocks, *Journal of Structural Geology*, **26**, (2004), 1727–1747.

Pickup, G.E., Ringrose, P.S., Corbett, P.W.M., Jensen, J.L. and Sorbie, K.S.: Geology, geometry and effective flow, *Petroleum Geoscience*, **1**, (1995), 37-42.

Sibson, R.H.: Fluid Flow Accompanying Faulting: Field Evidence and Models, in: Earthquake Prediction, Simpson, D. W. and Richards, P. G. (Ed.), 593-603, *American Geophysical Union*, Washington D. C., (1981).

Tchalenko, J.S.: Similarities between Shear Zones of Different Magnitudes, *Geological Society of America Bulletin*, **81,** (1970),1625-1640.

TerHeege, J.H.: Distribution and properties of faults and fractures in shales: Permeability model and implications for optimum flow stimulation by hydraulic fracturing, *50th US Rock Mechanics / Geomechanics Symposium 2016*, Houston, USA, (2016).

Torabi, A. and Berg, S.S.: Scaling of fault attributes: A review, *Marine and Petroleum Geology*, **28**, (2011), 1444-1460.

Van Wees, J.D., Kronimus, A., Van Putten, M., Pluymaekers, M.P.D., Mijnlieff, H., Van Hooff, P., Obdam, A. and Kramers, L.: Geothermal aquifer performance assessment for direct heat production - Methodology and application to Rotliegend aquifers, *Netherlands Journal of Geosciences*, **91**, (2012), 651-665.

Wibberley, C.A.J., Yielding, G. and Di Toro, G.: Recent advances in the understanding of fault zone internal structure: a review, in: The Internal Structure of Fault Zones: Implications for Mechanical and Fluid-Flow Properties, Wibberley, C.A.J., Kurz, W., Imber, J., Holdsworth, R.E., Collettini, C. (Ed.), **299**, 5–33, *The Geological Society of London*, London, (2008).

Wibberley, C.A.J. and Shimamoto, T.: Internal structure and permeability of major strike–slip fault zones: the Median Tectonic Line in W. Mie Prefecture, S. W. Japan, *Journal of Structural Geology*, **25**, (2003), 59–78.

Yielding, G., Freeman, B. and Needman, T.: Quantitative fault seal prediction, *American Association of Petroleum Geologists Bulletin*, **81**, (1997), 897–917.

Acknowledgements

The IMAGE project leading to part of this article received funding from the European Union’s FP7 research and innovation programme under grant agreement No 608553. The IMAGE project studies Integrated Methods for Advanced Geothermal Exploration.